Applied Energy 218 (2018) 520–532

Contents lists available at ScienceDirect

Applied Energy

journal homepage: www.elsevier.com/locate/apenergy

A decentralized trading algorithm for an electricity market with generation uncertainty

Shahab Bahrami[a,1], M. Hadi Amini[b,*]

[a] Department of Electrical and Computer Engineering, University of British Columbia, Vancouver, BC, Canada
[b] Department of Electrical and Computer Engineering, Carnegie Mellon University, Pittsburgh, PA, USA

HIGHLIGHTS

- A decentralized energy trading algorithm is proposed considering the integration of renewable energy resources.
- Our method optimizes the cost of load aggregators and profit of the generators.
- The proposed optimization problem minimizes as the risk of shortage in the renewable generation.
- A risk measure called the conditional-value-at-risk (CVaR) is used to model uncertainty of renewables.
- The simulation results validate the effectiveness of the proposed decentralized algorithm.

ARTICLE INFO

Keywords:
Renewable Energy Resources
Price-responsive load aggregator
Power market
Conditional value-at-risk (CVaR)
Generation uncertainty
Controllable load
Decentralized algorithm

ABSTRACT

The uncertainties in renewable power generators and the proliferation of price-responsive load aggregators make it a challenge for independent system operators (ISOs) to manage the energy trading in the power markets. Hence, a centralized framework for the energy trading market may not be remained practical for the ISOs mainly due to violating the privacy of different entities, i.e., load aggregators and generators. It can also suffer from the high computational burden in a market with a large number of entities. Instead, in this paper, we focus on proposing a *decentralized* energy trading framework enabling the ISO to incentivize the entities toward an operating point that jointly optimize the cost of load aggregators and profit of the generators, as well as the risk of shortage in the renewable generation. To address the uncertainties in the renewable resources, we apply a risk measure called the conditional value-at-risk (CVaR) with the goal of limiting the likelihood of high renewable generation shortage with a certain confidence level. Then by considering the risk attitude of the ISO and the generators, we develop a decentralized energy trading algorithm with some control signals that properly coordinate the entities toward the market operating point of the ISO's centralized approach. Simulation results on the IEEE 30-bus test system show that the proposed decentralized algorithm converges to the solution of the ISO's centralized problem in a timely fashion. Furthermore, the load aggregators can help their consumers reduce their electricity cost by 18% on average through managing their loads using locally available information. Meanwhile, the generators can benefit from 17.1% increase in their total profit through decreasing their generation cost.

1. Introduction

One of the foremost goals of the future smart grid is to provide the necessary infrastructures toward integration of renewable generators (e.g., wind turbine and photovoltaic (PV) panel) as the environmentally friendly alternatives for the fossil fuel-based power plants. Meanwhile, the infrastructure in the smart grid can facilitate the participation of the demand side in the energy management programs such as the demand response (DR) [1,2].

Independent system operators (ISOs) usually perform comprehensive analysis (e.g., optimal power flow and unit commitment) to optimally dispatch the available generation portfolio in order to supply the load demand. Nevertheless, there are challenges in performing energy market analysis in a centralized fashion, especially in a grid with

* Corresponding author. Department of Electrical and Computer Engineering, Carnegie Mellon University, Pittsburgh, PA 15213, USA.
E-mail addresses: shahab_bahrami@yahoo.com (S. Bahrami), hadi.amini@ieee.org (M.H. Amini).
URL: http://www.hadiamini.com (M.H. Amini).
[1] Shahab Bahrami graduated from the Department of Electrical and Computer Engineering, University of British Columbia in 2017.

https://doi.org/10.1016/j.apenergy.2018.02.157
Received 7 November 2017; Received in revised form 22 February 2018; Accepted 23 February 2018
Available online 22 March 2018
0306-2619/

Nomenclature

y_h arbitrary scaler y in time slot h.
$\boldsymbol{y}$ arbitrary vector $(y_h, h \in \mathscr{H})$.

Variables and parameters for generator j

$p_{j,h}^{\text{conv}}$ conventional unit's output power
$p_{j,h}^{\text{ren}}$ predicted renewable generation
$\widehat{p}_{j,h}^{\text{ren}}$ actual renewable generation
β_j confidence level of the generator

Variables and parameters for load aggregator i

$l_{i,h}$ total load demand
$\boldsymbol{x}_i$ profile of load demands
$\boldsymbol{x}_{a,i}$ demand profile of load a
$x_{a,i,h}$ demand of load a
$\boldsymbol{x}_{a,i}^{\text{des}}$ desirable profile of load a
$\mathscr{H}_{a,i}$ scheduling horizon of load a

Other variable and parameters

$\delta_{b,h}$ voltage phase angle of bus b
$p_{r,s}^{\max}$ maximum power flow limit for line $(r,s) \in \mathscr{L}$
$b_{r,s}$ admittance of line $(r,s) \in \mathscr{L}$
ϵ^q step size in iteration q

renewable generators and price-responsive load aggregators. First and perhaps most importantly, the centralized market analysis by the ISO can violate the entities' privacy in a competitive energy market, e.g., by revealing the demand information of the load aggregators and operational cost of the generators. Second, the uncertainty in the privately-owned renewable generators puts the generation-load balance at risk. Third, the centralized market analysis can be computationally difficult in large power grids, especially when the number of decision variables dramatically increases by participating the price-responsive load aggregators and small-scaled renewable generators in the competitive energy market.

There have been some efforts in the power system operation literature to tackle the above-mentioned challenges. Qadran et al. [3] studied the application of DR in combined gas networks and power systems. According to Drysdale et al. [4], the flexible load demand needs three major criteria for the participants: identifiability, accessibility, and being useful. We divide the related works into three threads. The first thread of the literature is concerned with the participation of the price-responsive loads in the DR programs and addresses the entities' privacy issues thorugh designing decentralized energy planning algorithms using the evolutionary game [5], stochastic game [6], Stackelberg game [7], dual decomposition method [8], multi-agent system [9], multi-agent systems [10,11], and hierarchical bidding [12]. These approaches, however, may not be easily implementable in practice, since they ignore the physical constraints imposed by the topology and operation of the power network. In order to achieve an accurate estimation of the load demand, a multi-time-scale method is developed in [13] that outperforms the available forecasting methods. The second thread of the literature is concerned with considering the power flow constraints in the decentralized system planning procedure using different techniques such as the primal-dual algorithm [14], convex relaxation [15–17], quadratic programming [18], alternating direction method of multipliers (ADMM) [19–21], diagonal quadratic approximation [22], and Lagrange relaxation method [23–25]. In these works, nevertheless, the uncertainty issues related to the integration of the renewable generators have remained as a primary challenge. The third thread of the literature is concerned with addressing the uncertainty issues by using chance-constrained optimization [26–28], successive constraint enforcement [29], fuzzy system [30], stochastic optimization [31,32], and risk management [33–37]. The proposed models include the power flow constraints and deal with the uncertainty issues. However, they are implemented in a centralized fashion, and thus cannot address the privacy and computational complexity concerns.

In this paper, we focus on extending the works in the above-mentioned threads of the literature by designing a decentralized energy trading algorithm in a day-ahead electricity market with renewable energy generators and active participation of load aggregators in the DR programs. The ISO, load aggregators, and generators use the smart grid's communication infrastructure to execute the proposed distributed algorithm and jointly optimize the profit (for the generators) from selling electricity and the cost (for load aggregators) of purchasing electricity. Each entity solves its own optimization problem using the locally available information. Hence, the privacy of each entity is preserved. Compared to our previous work [38], the main challenge is to consider the uncertainty in the renewable generation and design proper control signals among the ISO, generators, and load aggregators that enforce the proposed decentralized algorithm to converge to the optimal solution of the centralized problem of the ISO. The main contributions of this paper are as follows:

- *Risk evaluation*: Inspired by the works in [33,34], we deploy a penalty term based on the conditional value-at-risk (CVaR) into the objective functions of both the ISO's centralized problem and the generators' local problem in order to address the uncertainties of the renewable generation. It enables the generators with renewable plants to sell electricity and gain profit, while limiting the risk of high generation shortage within a certain confidence level. The ISO can also reduce the risk of generation-load mismatch based on its own risk attitude. We discuss how to deal with the different risk attitudes of the ISO and the generators. It is worth noting that the systemic-risk oriented methods for network fragility assessment in other types of multi-agent dynamical networks have been widely investigated by researchers in control network area [39,40].
- *Decentralized algorithm design*: To protect the privacy of the entities, as well as reducing the computational complexity, we propose a decentralized algorithm based on the Lagrange relaxation method [23,24] that can be executed by the entities to trade in the competitive energy markets. A load aggregator schedules the customers' loads, and a generator determines its risk minimizing generation level. Meanwhile, the ISO can meet the network physical constraints, thus achieving a triple-win result.
- *Performance evaluation*: Simulation results on a modified IEEE 30-bus test system show that the proposed decentralized algorithm provably converges to the optimal solution to the centralized problem of the ISO in about 45 iterations. The proposed algorithm also benefits both the load aggregators by reducing their cost by 18%, the generators by increasing their profit by 17.1% and decreasing the peak-to-average ratio (PAR) by 15%. When compared with the centralized approach, our algorithm has a significantly lower running time, as the entities can execute the algorithm in a parallel fashion.

The rest of this paper is organized as follows. Section 2 formulates the ISO's centralized problem. In Section 3, we propose a decentralized algorithm to determine the energy market equilibrium. Section 4 provides simulation results, followed by Section 5 that concludes the paper.

2. System model

Consider a day-ahead energy market with a set $\mathcal{I}$ of load aggregators and a set $\mathcal{J}$ of generators. The ISO is responsible for the safe operation of the power network during the energy trading horizon $\mathcal{H} = \{1,...,H\}$, where H is the number of time slots with an equal length, e.g., one hour. Load aggregator $i \in \mathcal{I}$ is responsible for saving money through scheduling the (controllable) load demands during the trading horizon $\mathcal{H}$ on behalf of its electricity consumers. Generator $j \in \mathcal{J}$ supplies electricity to the market to make profit. The load aggregators and generators use a two-way communication infrastructure to exchange necessary information with the ISO.

To avoid potential confusions, we assume that each bus has either a load aggregator or a generator. If a load aggregator and a generator are connected to the same bus, we divide that bus into two buses connected to each other through a line with zero impedance. If neither load aggregator nor generator is connected to a bus, we add a virtual load aggregator with zero demand to that bus. This assumption enables us to denote the set of buses by $\mathcal{I} \cup \mathcal{J}$ and refer a load aggregator or a generator by its bus number.

In the following, we discuss how the ISO can manage the energy trading market in a centralized fashion.

2.1. Centralized problem formulation for the ISO

The ISO may have a variety of different objectives in the energy market, while satisfying the operation constraints of the power grid. In this paper, we consider the objective of minimizing the *social cost* incorporated with the risk of generation shortage of the renewable generators during the trading horizon $\mathcal{H}$.

In the following parts, we will discuss the models of the generators, load aggregators, and the power network to formulate the ISO's centralized problem in the energy market.

2.1.1. Generator's model

Generator $j \in \mathcal{J}$ supplies the market with the generation profile $\boldsymbol{p}_j^{\text{conv}} = (p_{j,h}^{\text{conv}}, h \in \mathcal{H})$ of its conventional units. The generation cost of conventional units of generator j in time slot h can generally be modeled by an increasing convex function of output power $p_{j,h}^{\text{conv}}$ [41]. The class of quadratic generation cost functions is well-known in the literature [42]. We have

$$C_j(\boldsymbol{p}_j^{\text{conv}}) = \sum_{h\in\mathcal{H}} (a_{j2}(p_{j,h}^{\text{conv}})^2 + a_{j1}p_{j,h}^{\text{conv}} + a_{j0}), j \in \mathcal{J}, \tag{1}$$

where coefficients a_{j0},a_{j1}, and a_{j2} are nonegative coefficients such that the quadratic function becomes an increasing convex over the following feasible bounds for the output power:

$$p_j^{\min} \leqslant p_{j,h}^{\text{conv}} \leqslant p_j^{\max}, \quad j \in \mathcal{J}, h \in \mathcal{H}. \tag{2}$$

A generator can also setup renewable units that have (approximately) zero generation cost. If the ISO is responsible for determining the generation portfolio in the market, then it has uncertainty about the renewable generation profile of each generator $j \in \mathcal{J}$. In the underlying day-ahead market, the ISO considers the predicted generation profile $\boldsymbol{p}_j^{\text{ren}} = (p_{j,h}^{\text{ren}}, h \in \mathcal{H})$ such that the *risk* of deviation from the *actual* generation profile $\hat{\boldsymbol{p}}_j^{\text{ren}} = (\hat{p}_{j,h}^{\text{ren}}, h \in \mathcal{H})$ is minimized.

The ISO can tolerate the excessive renewable generation by simply preventing the excessive power from being injected to the grid. However, the scenario with generation shortage cannot be easily addressed by the ISO. The ISO can use risk measures such as the value-at-risk (VaR) and conditional value-at-risk (CVaR) to limit the risk of generation shortage within a confidence level [43]. Let $\Delta_{j,h}^{\text{ISO}}(p_{j,h}^{\text{ren}}, \hat{p}_{j,h}^{\text{ren}})$ denote the function that captures the generation shortage in time slot h for generator j. It is defined as

$$\Delta_{j,h}^{\text{ISO}}(p_{j,h}^{\text{ren}}, \hat{p}_{j,h}^{\text{ren}}) = [p_{j,h}^{\text{ren}} - \hat{p}_{j,h}^{\text{ren}}]^+, \quad j \in \mathcal{J}, h \in \mathcal{H}, \tag{3}$$

where $[\cdot]^+ = \max\{\cdot, 0\}$. Note that $\Delta_{j,h}^{\text{ISO}}(p_{j,h}^{\text{ren}}, \hat{p}_{j,h}^{\text{ren}})$ is a random variable, since the actual generation $\hat{p}_{j,h}^{\text{ren}}$ is a stochastic process. Under a given confidence level $\beta_j^{\text{ISO}} \in (0,1)$ and the predicted generation level $p_{j,h}^{\text{ren}}$ in time slot h, the VaR for generator j is defined as the minimum threshold $\alpha_{j,h}^{\text{ISO}}$, for which the probability of generation shortage of generator j being less than $\alpha_{j,h}^{\text{ISO}}$ is at least β_j^{ISO} [43]. That is,

$$\text{VaR}_{j,h}^{\beta_j^{\text{ISO}}}(p_{j,h}^{\text{ren}}) = \min\{\alpha_{j,h}^{\text{ISO}} \mid Pr(\Delta_{j,h}^{\text{ISO}}(\cdot) \leqslant \alpha_{j,h}^{\text{ISO}}) \geqslant \beta_j^{\text{ISO}}\}. \tag{4}$$

The VaR is non-convex, and thus it is difficult to be minimized. The CVaR is an alternative risk measure, which is convex and can be optimized using sampling techniques. The CVaR of the ISO associated with generator j in time slot h is defined as the expected value of $\Delta_{j,h}^{\text{ISO}}(\cdot)$ when only the values of $\Delta_{j,h}^{\text{ISO}}(\cdot)$ that are greater than or equal to $\text{VaR}_{j,h}^{\beta_j}(p_{j,h}^{\text{ren}})$ are considered [43]. That is,

$$\text{CVaR}_{j,h}^{\beta_j^{\text{ISO}}}(p_{j,h}^{\text{ren}}) = \text{E}\{\Delta_{j,h}^{\text{ISO}}(\cdot) | \Delta_{j,h}^{\text{ISO}}(\cdot) \geqslant \text{VaR}_{j,h}^{\beta_j^{\text{ISO}}}(p_{j,h}^{\text{ren}})\}. \tag{5}$$

From (5), the VaR is upper bounded by the CVaR, and hence minimizing the CVaR can results in a low VaR as well.

The expectation in (5) requires the probability distribution of the actual generation $\hat{p}_{j,h}^{\text{ren}}$, which may not be available in practice. For a predicted generation level $p_{j,h}^{\text{ren}}$, it is possible to *estimate* the CVaR in (5) by adopting the sample average approximation (SAA) technique [43]. Samples of the random variable $\hat{p}_{j,h}^{\text{ren}}$ for generator j can be observed from the historical record. Consider the set $\mathcal{K}_j = \{1,...,K_j\}$ of K_j samples of the random variable $\hat{p}_{j,h}^{\text{ren}}$. Let $p_{j,h}^{\text{ren},k}$ denote the k^{th} sample of $\hat{p}_{j,h}^{\text{ren}}$ for generator j in time slot h. The CVaR in (5) can be estimated by

$$\text{CVaR}_{j,h}^{\beta_j^{\text{ISO}}}(p_{j,h}^{\text{ren}}) \approx \min_{\alpha_{j,h}^{\text{ISO}}} \widetilde{\mathscr{C}}_{j,h}^{\beta_j^{\text{ISO}}}(p_{j,h}^{\text{ren}}, \alpha_{j,h}^{\text{ISO}}), \tag{6}$$

where

$$\widetilde{\mathscr{C}}_{j,h}^{\beta_j^{\text{ISO}}}(p_{j,h}^{\text{ren}}, \alpha_{j,h}^{\text{ISO}}) = \alpha_{j,h}^{\text{ISO}} + \sum_{k\in\mathcal{K}_j} \frac{[\Delta_{j,h}^{\text{ISO}}(p_{j,h}^{\text{ren}}, p_{j,h}^{\text{ren},k}) - \alpha_{j,h}^{\text{ISO}}]^+}{K_j(1-\beta_j^{\text{ISO}})}. \tag{7}$$

From the ISO's perspective, the CVaR for generator j over the trading horizon $\mathcal{H}$ is $\widetilde{\mathscr{C}}_j^{\beta_j^{\text{ISO}}}(\boldsymbol{p}_j^{\text{ren}}, \boldsymbol{\alpha}_j^{\text{ISO}}) = \sum_{h\in\mathcal{H}} \widetilde{\mathscr{C}}_{j,h}^{\beta_j^{\text{ISO}}}(p_{j,h}^{\text{ren}}, \alpha_{j,h}^{\text{ISO}})$.

2.1.2. Load aggregator's model

Load aggregator $i \in \mathcal{I}$ is responsible for managing the demand of its consumers. The total demand $l_{i,h} = \sum_{a\in\mathcal{A}_i} x_{a,i,h}$ of load aggregator i in time slot h involves the demands of a set $\mathcal{A}_i$ of different loads with different characteristics (e.g., uncontrollable and controllable loads). Load aggregator i decides on the feasible profile $\boldsymbol{x}_i$ that includes the demands $x_{a,i,h}$ of all loads $a \in \mathcal{A}_i$ in time slots $h \in \mathcal{H}$. In Appendix A, the operation constraints for the uncontrollable and controllable loads are discussed. Let $\mathcal{X}_i$ denote the feasible demand space defined by the operational constraints for load aggregator i. We have

$$\boldsymbol{x}_i \in \mathcal{X}_i, \quad i \in \mathcal{I}. \tag{8}$$

Scheduling the loads usually results in a discomfort cost for the consumers of the load aggregator i. The discomfort cost $\Omega_{a,i}(\boldsymbol{x}_{a,i})$ for load $a \in \mathcal{A}_i$ is due to deviating from desirable consumption profile $\boldsymbol{x}_{a,i}^{\text{des}} = (x_{a,i,h}^{\text{des}}, h \in \mathcal{H})$ to the scheduled consumption profile $\boldsymbol{x}_{a,i} = (x_{a,i,h}, h \in \mathcal{H})$. We assume that the discomfort cost $\Omega_{a,i}(\boldsymbol{x}_{a,i})$ is an increasing concave function of $\boldsymbol{x}_{a,i}$. The total discomfort cost for load aggregator i is $\Omega_i(\boldsymbol{x}_i) = \sum_{a\in\mathcal{A}_i} \Omega_{a,i}(\boldsymbol{x}_{a,i})$.

2.1.3. Power network model

As a neutral entity, the ISO uses the DC power flow model as an acceptable framework to determine the active power flow through the lines in transmission systems [44,45]. Considering the profile $\boldsymbol{\delta}$ of voltage phase angles for all buses in all time slots, we have:

$$l_{i,h} = -\sum_{(i,r)\in\mathscr{L}} b_{i,r}(\delta_{i,h}-\delta_{r,h}), \quad i\in\mathscr{I}, \quad h\in\mathscr{H}, \tag{9a}$$

$$p_{j,h}^{\text{conv}} + p_{j,h}^{\text{ren}} = \sum_{(j,r)\in\mathscr{L}} b_{j,r}(\delta_{j,h}-\delta_{r,h}), \quad j\in\mathscr{J}, \tag{9b}$$

$$|b_{r,s}(\delta_{r,h}-\delta_{s,h})| \leqslant p_{r,s}^{\max}, (r,s)\in\mathscr{L}, \quad h\in\mathscr{H}, \tag{9c}$$

$$\delta_{1,h} = 0, \quad h\in\mathscr{H}. \tag{9d}$$

Constraints (9a) and (9b) are the nodal power balance equations. Constraint (9c) is the line flow limit. In constraint (9d), bus 1 is considered as the slack bus.

2.1.4. ISO's centralized problem

For the ISO, we define the vector of decision variables as $\boldsymbol{\psi}^{\text{ISO}} = (\boldsymbol{p}_j^{\text{conv}}, \boldsymbol{p}_j^{\text{ren}}, \boldsymbol{\alpha}_j^{\text{ISO}}, \boldsymbol{x}_i, \delta, j\in\mathscr{J}, i\in\mathscr{I})$. As mentioned, we consider the objective of minimizing the social cost incorporated with the risk of generation shortage of the renewable units over the trading horizon $\mathscr{H}$. That is

$$f^{\text{ISO}}(\boldsymbol{\psi}^{\text{ISO}}) = \sum_{i\in\mathscr{I}} \Omega_i(\boldsymbol{x}_i) + \sum_{j\in\mathscr{J}} (C_j(\boldsymbol{p}_j^{\text{conv}}) + \vartheta^{\text{c}} \widetilde{\mathscr{C}}_j^{\beta_j^{\text{ISO}}}(\boldsymbol{p}_j^{\text{ren}}, \boldsymbol{\alpha}_j^{\text{ISO}})), \tag{10}$$

where ϑ^{c} is a nonegative weighting coefficient in "$"/MW h. A higher value of ϑ^{c} leads to a higher weight for the CVaR term, and thus the ISO becomes more risk averse, thus prefers a lower value of renewable energy shortage in the network. We formulate the ISO's centralized problem as

$$\underset{\boldsymbol{\psi}^{\text{ISO}}}{\text{minimize}}\ f^{\text{ISO}}(\boldsymbol{\psi}^{\text{ISO}}) \tag{11a}$$

$$\text{subject to constraints (2),(8) and (9).} \tag{11b}$$

In Theorem 1, we discuss the existence and uniqness of the solution for problem (11).

Theorem 1. *If the ISO's centralized problem in (11) has a feasible point, then the optimal solution exists and is unique.*

The proof can be found in Appendix B. We note that the optimal solution to the ISO's centralized problem (11) with the approximated CVaR converges exponentially fast to the optimal solution of the ISO's problem with the exact CVaR in (5) as the sample size K_j increases. The proof of this claim is beyond the scope of this paper. Interested readers are referred to [46] for the detailed analysis of the generic problem tackled using the theory of large deviations.

To solve the centralized problem in (11), the ISO requires full information about the load aggregators' discomfort cost and the conventional generators' operation cost. However, this information may not be available to the ISO in practice. Furthermore, solving problem (11) can be computationally difficult in large power networks. Instead, we develop a decentralized algorithm, in which the ISO provides the load aggregators and generators with some control signals to motivate them towards the optimal solution to problem (11).

3. Energy market interactions

The ISO has no*direct* control over the generators' and load aggregators' behavior. Alternatively, the ISO provides the entities with sufficient access to the day-ahead energy market to optimally determine their own generation and load demand.

3.1. Generator's and load aggregator's local problems

In the underlying day-ahead market, the ISO purchases the total output power $p_{j,h}^{\text{conv}} + p_{j,h}^{\text{ren}}$ of generator j with the prices $\boldsymbol{\rho}_j = (\rho_{j,h}, h\in\mathscr{H})$. Nevertheless, generator j has uncertainty about its renewable generation profile $\boldsymbol{p}_j^{\text{ren}}$. To prevent the generators from non-credible high renewable generation offers in the day-ahead market, the ISO charges generator j with renewable units by the price $\theta_{j,h}^1, h\in\mathscr{H}$ ($/kW h), if its actual generation $\widehat{p}_{j,h}^{\text{ren}}$ is *lower* than its offer $p_{j,h}^{\text{ren}}$. The ISO also charges generator j with a base payment/reward $\theta_{j,h}^2, h\in\mathscr{H}$ ($), which plays a role either as a penalty payment for renewable generation if $\theta_{j,h}^2 > 0$ or as an incentive reward for renewable generation $\theta_{j,h}^2 < 0$. In Section 3.2, we will discuss the conditions for positive and negative $\theta_{j,h}^2$.

Generator j aims to minimize the *risk* of deviation from the *actual* generation profile $\widehat{\boldsymbol{p}}_j^{\text{ren}}$, and uses risk measure CVaR to limit the penalty for the generation shortage. Let $\Delta_{j,h}(p_{j,h}, \widehat{p}_{j,h})$ denote a function that captures the penalty for the generation shortage in time slot h for generator j with renewable units[43]. It is defined as

$$\Delta_{j,h}(p_{j,h}^{\text{ren}}, \widehat{p}_{j,h}^{\text{ren}}) = \theta_{j,h}^1 [p_{j,h}^{\text{ren}} - \widehat{p}_{j,h}^{\text{ren}}]^+ + \theta_{j,h}^2, \quad j\in\mathscr{J}. \tag{12}$$

We would like to emphasize that function $\Delta_{j,h}(p_{j,h}^{\text{ren}}, \widehat{p}_{j,h}^{\text{ren}})$ in (12) is different from function $\Delta_{j,h}^{\text{ISO}}(p_{j,h}^{\text{ren}}, \widehat{p}_{j,h}^{\text{ren}})$ in (3). In fact, generator j cares about the penalty for the generation shortage, but the ISO cares about the amount of generation shortage. Hence, the objectives of the ISO and generators in lowering the risk of generation shortage is different.

Similar to the approach in Section 2.1, we can approximate the $\text{CVaR}_{j,h}^{\beta_j}(p_{j,h}^{\text{ren}})$ associated with generator j with confidence level β_j by

$$\text{CVaR}_{j,h}^{\beta_j}(p_{j,h}^{\text{ren}}) \approx \min_{\alpha_{j,h}} \widetilde{\mathscr{C}}_{j,h}^{\beta_j}(p_{j,h}^{\text{ren}}, \alpha_{j,h}), \tag{13}$$

where

$$\widetilde{\mathscr{C}}_{j,h}^{\beta_j}(p_{j,h}^{\text{ren}}, \alpha_{j,h}) = \alpha_{j,h} + \sum_{k\in\mathscr{K}_j} \frac{[\Delta_{j,h}(p_{j,h}^{\text{ren}}, p_{j,h}^{\text{ren},k}) - \alpha_{j,h}]^+}{K_j(1-\beta_j)}. \tag{14}$$

We note that $\widetilde{\mathscr{C}}_{j,h}^{\beta_j}(p_{j,h}^{\text{ren}}, \alpha_{j,h})$ in (14) is different from $\widetilde{\mathscr{C}}_{j,h}^{\beta_j^{\text{ISO}}}(p_{j,h}^{\text{ren}}, \alpha_{j,h}^{\text{ISO}})$ in (7) as the confidence level β_j of generator j in the energy market can be different from the confidence level β_j^{ISO} of the ISO in the centralized approach. The CVaR for generator j over the trading horizon $\mathscr{H}$ is $\widetilde{\mathscr{C}}_j^{\beta_j}(\boldsymbol{p}_j^{\text{ren}}, \boldsymbol{\alpha}_j) = \sum_{h\in\mathscr{H}} \widetilde{\mathscr{C}}_{j,h}^{\beta_j}(p_{j,h}^{\text{ren}}, \alpha_{j,h})$.

We define decision vector $\boldsymbol{\varphi}_j = (\boldsymbol{p}_j^{\text{conv}}, \boldsymbol{p}_j^{\text{ren}}, \boldsymbol{\alpha}_j)$ for generator j. The objective of a generator is to maximize its profit π_j^{gen}, which is the revenue from selling electricity in the market with prices $\rho_{j,h}, h\in\mathscr{H}$ minus the generation cost and the financial risk CVaR in (14). The profit of generator $j\in\mathscr{J}$ is obtained as follows:

$$\pi_j^{\text{gen}}(\boldsymbol{\varphi}_j) = \sum_{h\in\mathscr{H}} \rho_{j,h}(p_{j,h}^{\text{conv}} + p_{j,h}^{\text{ren}}) - C_j^{\text{conv}}(\boldsymbol{p}_j^{\text{conv}}) - \widetilde{\mathscr{C}}_j^{\beta_j}(\boldsymbol{p}_j^{\text{ren}}, \boldsymbol{\alpha}_j). \tag{15}$$

Let Φ_j denote the feasible space defined by constraint (2) for generator j. The local optimization problem for generator $j\in\mathscr{J}$ is

$$\underset{\boldsymbol{\varphi}_j\in\Phi_j}{\text{maximize}}\ \pi_j^{\text{gen}}(\boldsymbol{\varphi}_j) \tag{16}$$

Each load aggregator i aims to determine the profile $\boldsymbol{x}_i = (\boldsymbol{x}_{a,i}, a\in\mathscr{A}_i)$ of power demands over all loads by minimizing its total cost $C_i^{\text{agg}}(\boldsymbol{x}_i)$, which includes the discomfort cost $\Omega_i(\boldsymbol{x}_i)$ and the payment to the ISO to meet the total demand $l_{i,h} = \sum_{a\in\mathscr{A}_i} x_{a,i,h}$. In the energy market, the ISO provides each load aggregator i with the electricity prices $\boldsymbol{\rho}_i = (\rho_{i,h}, h\in\mathscr{H})$. For $i\in\mathscr{I}$, we have

$$C_i^{\text{agg}}(\boldsymbol{x}_i) = \Omega_i(\boldsymbol{x}_i) + \sum_{h\in\mathscr{H}} \rho_{i,h}\left(\sum_{a\in\mathscr{A}_i} x_{a,i,h}\right). \tag{17}$$

Load aggregator $i\in\mathscr{I}$ solves the following optimization problem:

$$\underset{\boldsymbol{x}_i\in\mathscr{X}_i}{\text{minimize}}\ C_i^{\text{agg}}(\boldsymbol{x}_i) \tag{18}$$

3.2. Market equilibrium and price signals design

The decision vector of the load aggregator i is the load profile $\boldsymbol{x}_i$ and the decision vector for generator j is $\boldsymbol{\varphi}_j = (\boldsymbol{p}_j^{\text{conv}}, \boldsymbol{p}_j^{\text{ren}}, \boldsymbol{\alpha}_j)$. The ISO influences the entities by using the nodal prices $\boldsymbol{\rho} = (\rho_b, b \in \mathscr{I} \cup \mathscr{J})$ and the penalties $\boldsymbol{\theta} = ((\theta_j^1, \theta_j^2), j \in \mathscr{J})$ for renewable generators. The energy market equilibrium is defined as follows:

Definition 1. (Energy Market Equilibrium): Under the given vectors $\boldsymbol{\rho}$ and $\boldsymbol{\theta}$, the operating point $\mathscr{E}^{\star}_{\boldsymbol{\rho},\boldsymbol{\theta}} = (\boldsymbol{x}_i^{\star}, i \in \mathscr{I}, \psi_j^{\star}, j \in \mathscr{J})$ is the energy market equilibrium if the vectors $\boldsymbol{x}_i^{\star}$ and $\psi_j^{\star}$ are the optimal solutions to local problems (16) and (18) for generator $j \in \mathscr{J}$ and load aggregator $i \in \mathscr{I}$, respectively.

The ISO aims to determine vectors $\boldsymbol{\rho}$ and $\boldsymbol{\theta}$ such that the market equilibrium $\mathscr{E}^{\star}_{\boldsymbol{\rho},\boldsymbol{\theta}}$ coincides with the optimal solution to its centralized problem (11). The idea is to formulate the *dual problem* of the ISO's problem (11) in order to decompose problem (11) into subproblems corresponds to the generators and load aggregators. Then, we design vectors $\boldsymbol{\rho}$ and $\boldsymbol{\theta}$ such that the solution to the subproblems become the same as the solutions to local problems (18) and (16).

The dual problem of the ISO's centralized problem is formulated in Eq. (26) of Appendix C. We emphasize that the centralized problem (11) is strictly convex with linear constraints, and hence, the strong duality gap condition (Slater's condition) is satisfied if a feasible solution exists (see [47, Proposition 5.2.1]). That is, the optimal solution to the dual problem (26) is equal to the optimal solution to the ISO's centralized problem (11) [47, chapter 6].

For the ISO's centralized problem (11), we define the following Lagrange multipliers:

- $\lambda_{i,h}^{\text{agg}}, i \in \mathscr{I}, h \in \mathscr{H}$: Lagrange multiplier associated with the equality constraint (9a).
- $\lambda_{j,h}^{\text{gen}}, h \in \mathscr{H}, j \in \mathscr{J}$: Lagrange multiplier associated with the equality constraint (9b).

Furthermore, we define variable $\gamma_{j,h}^{\text{ISO},k} \in \{0,1\}$ as the indicator whether $[\Delta_{j,h}^{\text{ISO}}(p_{j,h}^{\text{ren}}, p_{j,h}^{\text{ren},k}) - \alpha_{j,h}^{\text{ISO}}]^+$ is zero or positive.

In the following theorem, we state our main result for designing the price signals.

Theorem 2. *The equilibrium of the energy market coincides with the unique solution to the ISO's centralized problem in (11) iff for $i \in \mathscr{I}, j \in \mathscr{J}, h \in \mathscr{H}$, the ISO sets*

$$\rho_{i,h}^{*} = \lambda_{i,h}^{\text{agg},*}, \tag{19a}$$

$$\rho_{j,h}^{*} = -\lambda_{j,h}^{\text{gen},*}, \tag{19b}$$

$$\theta_{j,h}^{1,*} = \vartheta^{c}\frac{1-\beta_j}{1-\beta_j^{\text{ISO}}}, \tag{19c}$$

$$\theta_{j,h}^{2,*} = \left[1 - \left(\frac{\vartheta^{c}(1-\beta_j)}{1-\beta_j^{\text{ISO}}} + \frac{(\vartheta^{c}-1)(1-\beta_j)}{\frac{1}{K_j}\sum_{k\in\mathscr{K}_j}\gamma_j^{\text{ISO},k,*}}\right)\right]\alpha_{j,h}^{*}. \tag{19d}$$

The proof of Theorem 2 can be found in Appendix C.

Remark 1. The control signals in (19a)–(19d) are bounded, i.e., the Lagrange multipliers are finite and the term $\sum_{k\in\mathscr{K}_j}\gamma_j^{\text{ISO},k,*}$ is not zero.

Now we discuss the intuition behind the price signals in (19a)–(19d). The Lagrange multipliers $\lambda_{i,h}^{\text{agg}}, i \in \mathscr{I}, h \in \mathscr{H}$ are nonnegative, because increasing $\sum_{(i,r)\in\mathscr{L}} b_{i,r}(\delta_{i,h} - \delta_{r,h})$ requires decreasing the load demand in bus i. A nonnegative Lagrange multiplier motivates load aggregator i toward reducing its load demand. In other words, in (19a), the ISO *charges* the load aggregators with price $\lambda_{i,h}^{\text{agg}}$.

The Lagrange multipliers $\lambda_{j,h}^{\text{gen}}, h \in \mathscr{H}, j \in \mathscr{J}$ are nonpositive, because increasing $\sum_{(j,r)\in\mathscr{L}} b_{j,r}(\delta_{j,h} - \delta_{r,h})$ requires increasing the generation in bus j. A nonpositive Lagrange multiplier motivates generator j toward increasing its generation. In other words, in (19b), the ISO *purchases* electricity from the generators with price $-\lambda_{j,h}^{\text{gen}}$.

The ISO penalizes the generators with renewable units by the prices $\theta_{j,h}^1, j \in \mathscr{J}, h \in \mathscr{H}$ in (19c) for the generation shortage. It also charges the generators with renewable units with amount of $\theta_{j,h}^2, j \in \mathscr{J}, h \in \mathscr{H}$ in (19d). We discuss the intuition behind the values of $\theta_{j,h}^1$ and $\theta_{j,h}^2$ by an illustrative example. Consider a scenario, in which $\vartheta_c > 1$ and the ISO is more risk averse than generator j, i.e., $\beta_j^{\text{ISO}} > \beta_j$. The ISO aims to motivate generator j to offer its renewable generation with a limited risk of generation shortage. Thus, the ISO sends the price signal $\theta_{j,h}^1 = \vartheta^{c}\frac{1-\beta_j}{1-\beta_j^{\text{ISO}}} > \vartheta^{c}$ to generator j. Furthermore, the ISO obtains $1 - \left(\frac{\vartheta^{c}(1-\beta_j)}{1-\beta_j^{\text{ISO}}} + \frac{(\vartheta^{c}-1)(1-\beta_j)}{\frac{1}{K_j}\sum_{k\in\mathscr{K}_j}\gamma_j^{\text{ISO},k}}\right)$ as a negative coefficient for the threshold cost $\alpha_{j,h}$ in (19d). Hence, the ISO motivates a higher value of the threshold cost $\alpha_{j,h}$ for generator j, which implies that the ISO motivates generator j to become more risk averse in the market.

By using the price signals, in (19a)–(19d), the ISO can manipulate the market equilibrium to be the same as the solution to its centralized problem (11). It suggests a decentralized algorithm for energy trading in the market.

3.3. Decentralized algorithm design

In a decentralized algorithm, the load aggregators, generators and ISO interact with each other in an iterative fashion. We first discuss the rationale of different entities. In the underlying market, each generator j naturally aims to maximize its profit from selling electricity. It solves the local problem (16) under the given price signals from the ISO. Each load aggregator i naturally aims to minimize the cost of purchasing electricity, and hence, it solves the local problem (18). The ISO receives observes the energy demand/supply from the load aggregators/generators, it provides the entities with the price signals in (19a)–(19d). Next, generators and load aggregators update their decisions by solving their local problems. This procedure continues until convergence to the market equilibrium. In Theorem 2, we have shown that the market equilibrium coincides with what the ISO wants from its centralized approach. Hence, it satisfies the ISO's expectations too.

Algorithm 1 describes the interactions among the load aggregators, generators, and ISO. Let q denote the iteration index. Algorithm 1 involves the initiation phase and the market trading phase.

Initiation phase: Lines 1–4 describe the initiation phase.

Market trading phase: The loop involving Lines 5–14 describes the market trading phase, in which the load aggregators, generators and ISO update their decision variables in an iterative fashion. This phase includes the following parts:

(a) *Information exchange:* In Line 6, each load aggregator i computes its load demand $l_{i,h}^q$ in time slot $h \in \mathscr{H}$ and sends its demand profile $\boldsymbol{l}_i^q$ to the ISO via the communication network. In Line 7, each generator j sends its decision profile $\boldsymbol{\varphi}_j^q = (\boldsymbol{p}_j^{\text{conv},q}, \boldsymbol{p}_j^{\text{ren},q}, \boldsymbol{\alpha}_j^q)$ to the ISO.

(b) *ISO's update:* Let $\boldsymbol{\Lambda} = (\lambda_{i,h}^{\text{agg}}, \lambda_{j,h}^{\text{gen}}, i \in \mathscr{I}, j \in \mathscr{J}, h \in \mathscr{H})$ denote the vector of Lagrange multipliers. In Line 8, when the ISO receives the updated information from the entities, it obtains the updated values of the bus voltage angles δ^{q+1}, as well as the vector of Lagrange multipliers $\boldsymbol{\phi}^{\text{ISO},q+1}$ using the gradient of the Lagrangian dual function $f_{\text{Dual}}^{\text{ISO}}(\boldsymbol{\delta}, \boldsymbol{\Lambda})$, which is given in (25) in Appendix C. We have

$$\boldsymbol{\delta}^{q+1} = \boldsymbol{\delta}^{q} + \epsilon^{q}\ \nabla_{\boldsymbol{\delta}} f_{\text{Dual}}^{\text{ISO}}(\boldsymbol{\delta}^{q}, \boldsymbol{\Lambda}^{q}), \tag{20a}$$

$$\boldsymbol{\Lambda}^{q+1} = \boldsymbol{\Lambda}^{q} + \epsilon^{q}\ \nabla_{\boldsymbol{\Lambda}} f_{\text{Dual}}^{\text{ISO}}(\boldsymbol{\delta}^{q}, \boldsymbol{\Lambda}^{q}), \tag{20b}$$

where ∇ is the gradient operator. The ISO also determines the updated values of binary variables $\gamma_{j,h}^{\mathrm{ISO},k,q}$ by taking into account the updated value of $[\Delta_{j,h}^{\mathrm{ISO}}(p_{j,h}^{\mathrm{ren},q},p_{j,h}^{\mathrm{ren},k})-\alpha_{j,h}^{q}]^{+}$ for each sample $k \in \mathscr{K}$ of renewable unit $j \in \mathscr{J}$.

In Line 9, the ISO uses the results of Theorem 2 to compute the updated values of the nodal prices ρ^{q+1} and penalties θ^{q+1} from (19a)–(19d). The ISO communicates the above price signals to the corresponding load aggregator and generator.

Algorithm 1. Decentralized Energy Trading Algorithm.

• **Initiation Phase:**

1: Set $q := 1$ and $\xi := 10^{-3}$.

2: Each load aggregator i randomly initializes its load profile $\boldsymbol{x}_i^1$.

3: Each generator j randomly initializes its profile $\boldsymbol{\varphi}_j^1$ and sends β_j to the ISO.

4: The ISO initializes the profiles of voltage angles $\boldsymbol{\delta}^1$ and Lagrange multipliers $\boldsymbol{\Lambda}^1$.

• **Market Trading Phase:**

5: **Repeat**

(a) *Information Exchange*

6: Each load aggregator i determines its total load demand $l_{i,h}^q, h \in \mathscr{H}$ and sends its demand profile $\boldsymbol{l}_i^q$ to the ISO.

7: Each generator j sends its decision profile $\boldsymbol{\varphi}_j^q$ to the ISO.

(b) *ISO's Update*

8: ISO updates the voltage angles $\boldsymbol{\delta}^q$ and the vector of Lagrange multipliers $\boldsymbol{\Lambda}^q$ according to (20a) and (20b), respectively. The ISO also determines the updated values of binary variables $\gamma_{j,h}^{\mathrm{ISO},k,q}$.

9: ISO broadcasts the updated nodal price ρ^{q+1} and penalties θ^{q+1} obtained from (19a)–(19d) to the entities.

(c) *Generator's Update*

10: Each generator j updates its decision vector $\boldsymbol{\varphi}_j^q$ by solving local problem (16).

(d) *Load Aggregator's Update*

11: Each load aggregator i updates its load profile $\boldsymbol{x}_i^q$ by solving local problem (18).

(e) *Step Size Update*

12: The step size ϵ^q is updated.

13: The iteration is updated, $q := q + 1$.

14: **Until** $||\boldsymbol{\delta}^q - \boldsymbol{\delta}^{q-1}|| \leqslant \xi$.

(c) *Generator's update:* When generator j receives the control signals $\rho_{j,h}^{q+1}$ and $\theta_{j,h}^{q+1}, h \in \mathscr{H}$ from the ISO, in Line 10, it updates its decision vector $\boldsymbol{\varphi}_j^q = (\boldsymbol{p}_j^{\mathrm{conv},q}, \boldsymbol{p}_j^{\mathrm{ren},q}, \boldsymbol{\alpha}_j^q)$ by solving its local problem in (16). It is a quadratic program with linear constraints and can be solved efficiently by the generator.

(d) *Load aggregator's update:* When load aggregator i receives the control signals $\rho_{i,h}^{q+1}, h \in \mathscr{H}$ from the ISO, in Line 11, it updates its load profile $\boldsymbol{x}_i^q$ by solving its local problem in (18), which is a quadratic program with linear constraints and can be solved efficiently.

(e) *Step size update:* We recommend a nonsummable diminishing step size with conditions $\lim_{q\to\infty} \epsilon^q = 0, \sum_{q=1}^{\infty} \epsilon^q = \infty$, and $\sum_{q=1}^{\infty} (\epsilon^q)^2 < \infty$ for the ISO's update. One example is $\epsilon^q = \frac{1}{a+bq}$, where a and b are positive constants. In Line 12, the step size is updated.

Remark 2. For the stopping criterion in Line 13, we have used the convergence of the voltage angles, since they depend on the generation and load level at all buses. Hence, the convergence of the voltage angles implies the convergence of all generators' and load aggregators' decision variables.

Remark 3. In the future smart grid, the entities are equipped with energy management system (EMS), which is responsible for smart decision making on behalf of the entities. Hence, Algorithm 1 can be executed in an autonomous fashion. In Section 4, we show that Algorithm 1 can converge to the market equilibrium in a reasonable number of iterations for the underlying day-ahead electricity markets. In practical applications, the ISO broadcasts the price signals to the

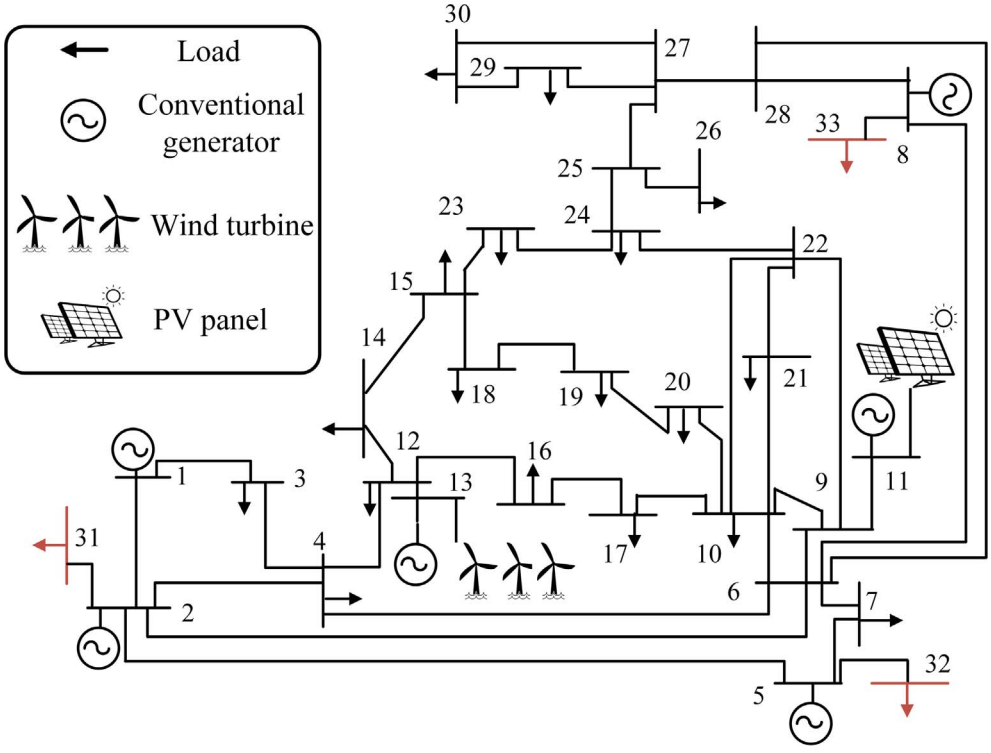

Fig. 1. IEEE 30-bus test system with 6 generators and 21 load aggregators. The generator in bus 11 also uses PV panel and the generator in bus 13 uses wind turbine to generate electricity in addition to the conventional units.

entities in each iteration, and then the entities communicate their energy demand/supply to the ISO. Hence, the number of iterations of Algorithm 1 can be interpreted as the number of message exchange among the entities and ISO over the available communication infrastructure in the smart grid.

4. Performance evaluation

In this section, we evaluate the performance of our proposed decentralized algorithm on an IEEE 30-bus test system shown in Fig. 1 with 6 generators and 21 load aggregators.

4.1. Simulation setup

The data for the analyzed test system and the cost function of generators are provide in [48]. Since buses 2,5, and 8 have generator and load aggregator in the original test system, we introduce the new virtual buses 31,32, and 33 for the load aggregators as shown in Fig. 1. The trading horizon is one day with $H = 24$ one-hour time slots. Unless stated otherwise, the weight coefficient in the ISO's objective function (10) is set to $\vartheta^c = 2$ ($/MW h) and the confidence level of the ISO for generator j is set to $\beta_j^{\text{ISO}} = 0.9$.

To obtain different baseload patterns for the load aggregators, we propose to use a load pattern for about 5 million consumers (which includes residential, commercial, and industrial consumers) from Ontario, Canada power grid database [49] from November 1 to November 21 2016. Without loss of generality, we scale the load pattern for each bus, such that the average baseload becomes equal to 60% of the load demand of that bus in [48]. In order to simulate the controllable load demand of each bus, we randomly generate the *desirable* load profile of 500–1000 controllable loads of types 1 and 2 with average demand of 2–15 kW at each bus. Limits $x_{a,i,h}^{\max}$ and $x_{a,i,h}^{\min}$ for a controllable load a in bus i are set to ± 30% of the desirable demand of that load in time slot h. Limits $X_{a,i}^{\max}$ and $X_{a,i}^{\min}$ for a controllable load a in bus i are set to ± 5% of the desirable total energy demand of that load. The discomfort coefficients $\omega_{a,i}$ and $\omega_{a,i,h}, h \in \mathscr{H}$ for each controllable load a are randomly chosen from a truncated normal distribution, which is lower bounded by zero, has a mean value of $\omega_i^{\text{avg}} = 15$ cents/(kW h)^2, and a standard deviation of 5 cents/(kW h)^2. The discomfort coefficients $\omega'_{a,i,h}, h \in \mathscr{H}$ for each controllable load a of type 2 are set to 50 cents/(kW h)^2.

We assume that generators in buses 11 and 13 have PV panel and wind turbine, respectively, in addition to their conventional units. The confidence levels of these generators are $\beta_{11} = \beta_{13} = 0.8$. To obtain the samples for the output power of the wind turbine and PV panel, we use the available historical data from Ontario, Canada power grid database [49], from November 1 to November 21 2016. Without loss of generality, for each renewable unit, we scale down the historical data, such that the average output power over the historical data becomes equal to 4 MW.

The step size is $\epsilon^q = \frac{1}{10+0.2q}$. We perform simulations using Matlab R2016b in a PC with processor Intel(R) Core(TM) i7-3770 K CPU@ 3.5 GHz.

4.2. Load aggregators' decision making

2) Load aggregators: Each load aggregator executes Algorithm 1 to modify the load demand of its users. For the *benchmark scenario*, we consider a system without renewable units and load management. Fig. 2 shows the load profile of the load aggregators in buses 17,30,31 (the load in bus 2), 33 (the load in bus 5). Peak shaving can be observed in the load profiles. Results for the load aggregators verify that by deploying the decentralized Algorithm 1 to manage the load demands, the peak load is reduced by 16.5% on average over all load aggregators. Load management is performed with the goal of reducing the total cost in (17). The simulations are performed several times with two different mean values for the discomfort coefficients $\omega_{a,i}$ and $\omega_{a,i,h}, h \in \mathscr{H}$ of the load aggregators. We provide the average results. Interestingly, Fig. 3 shows that the total cost in (17) of the load aggregators in different buses is lower (by about 18%) when the scaling coefficients ω_i^{avg} are lower, as the load aggregators can benefit from the price fluctuations by scheduling their load demand to the hours with lower price values.

4.3. Renewable generators' decision making

Generator 11 has a PV panel and generator 13 has a wind turbine in addition to their conventional units. Recall that these generators sell the *predicted* output power of the renewable units in the day-ahead market, and pay a penalty for their generation shortage in real time. According to Algorithm 1, the generators use the historical data of the renewable resources and respond to the control signals (19b)–(19d) to determine the amount of power that they plan to sell in the market. Fig. 4 shows the historical data and the predicted output power of the PV panel in bus 11 and the wind turbine in bus 13 for the confidence levels $\beta_{11} = \beta_{13} = 0.8$. The obtained presumed output power will have the lowest risk in the day-ahead market for these generators. Two parameters affect the predicted output power of a generator with a renewable unit: the value of the weight coefficient ϑ^c in the ISO's objective function (10) and the values of confidence levels β_j (set by generator j) and β_j^{ISO} (set by the ISO). The penalty $\theta_{j,h}^1$ in (19c) for the generation shortage increases when ϑ^c increases. That is, when the risk-averse ISO puts a higher weight on the risk of generation shortage, it assigns a larger penalty. Fig. 5 (*a*) (for bus 11) and Fig. 5 (*b*) (for bus 13) show that a larger coefficient ϑ^c enforces the generators to offer a lower renewable generation in the market during most of the times.

Following the similar manner, Eq. (19c) implies that when $\beta_j > \beta_j^{\text{ISO}}$,

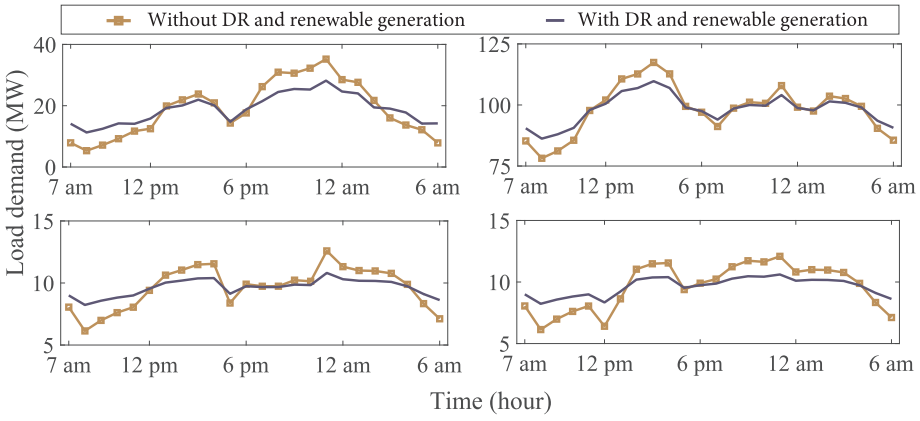

Fig. 2. Load demand profiles over 24 h in buses 31 (up-left), 32 (up-right), 17 (down-left), and 30 (down-right) with and without DR and renewable generators.

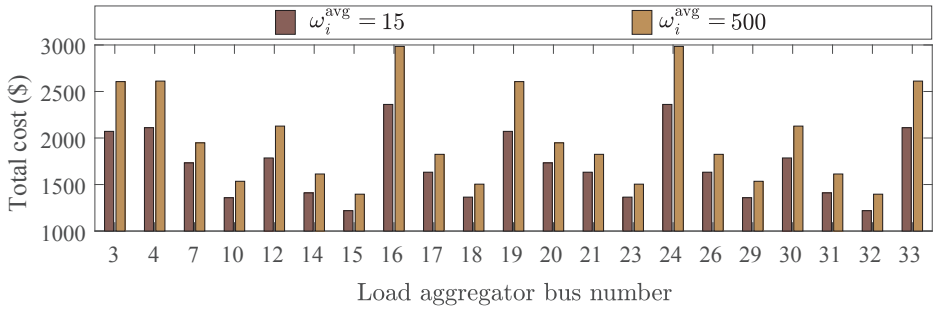

Fig. 3. The load aggregator's cost with low and high discomfort cost's scaling coefficients.

i.e., generator j is more risk-averse than the ISO, then the ISO reduces penalty $\theta^1_{j,h}$ by factor $\frac{1-\beta_j}{1-\beta_j^{ISO}} < 1$. If $\beta_j < \beta_j^{ISO}$, i.e., generator j is more risk-taker than the ISO, then the ISO increases penalty $\theta^1_{j,h}$ by $\frac{1-\beta_j}{1-\beta_j^{ISO}} > 1$ to limit the likelihood of generation shortage.

4.4. Conventional generators' decision making

The generators with conventional units can benefit from the market by reducing the PAR of the aggregate demand when the load aggregators schedule their load demands. For instance, Fig. 6 shows that the generation profile of the conventional units in bus 11 and 13 becomes smoother with scheduling the load demands. In other words, as the demand profiles in different buses change toward a profile with a lower peak demand, the required power generation follows the same trend. In order to quantify the impact of the DR program on the generation profile, we provide the average value of the PAR for different scenarios with and without DR program in Fig. 7. Results show the reduction in PAR for the generators by 15% on average. The reduction in the PAR results in a lower generation cost for the generators. Fig. 8 shows the profit (revenue minus cost) for the generators with and without DR program. The profit of the generators increases by 17.1% on average when the load aggregators schedule their loads. In order to complete the discussion, we consider different discomfort cost coefficients $\omega_i^{avg}, i \in \mathscr{I}$ for the load aggregators and report the average profit of generators in Fig. 9. It is interesting that the scenario with the most flexible load demands (i.e., $\omega_i^{avg} = 0$) does not lead to the maximum profit for the generators, though the generation cost of the generators is lower in this scenario. The reason is that a higher load flexibility will flatten the load profiles, which reduces the price values, and thus revenue of the generators. The reduction in the revenue can be more than the reduction in the costs. The maximum profit is achieved for $\omega_i^{avg} = 28.2$ cents/(kW h)^2, for which the load aggregators are neither too flexible nor too inflexible in the load scheduling.

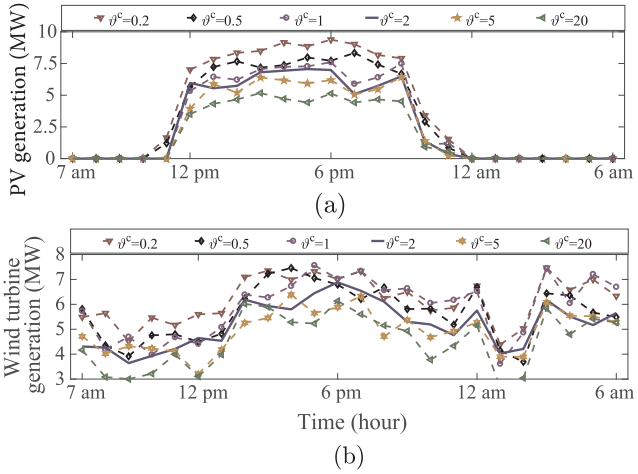

Fig. 5. The predicted output power of (a) the PV panel in bus 11, and (b) the wind turbine in bus 13 for different values of coefficient ϑ^c.

4.5. Price signals interpretation

We study the interpretation behind price signals in (19a)–(19d) in our case study. Fig. 10(a) shows the *average* Lagrange multipliers $E\{\lambda^{agg}_{i,h}\}$ for load aggregator i and $E\{\lambda^{gen}_{j,h}\}$ for generator j during the trading horizon $\mathscr{H}$. We can observe that $E\{\lambda^{agg}_{i,h}\}$ are positive, i.e., the ISO charges the load aggregators with average price $E\{\lambda^{agg}_{i,h}\}$. We can also observe that $E\{\lambda^{gen}_{j,h}\}$ are negative, i.e., the ISO pays the generators with average price $E\{\lambda^{gen}_{j,h}\}$.

Generators in buses 11 and 13 have the confidence levels $\beta_{11} = \beta_{13} = 0.8$. The confidence level of the ISO is $\beta_{ISO} = 0.9$. Hence, for $\vartheta^c = 2$ \$/MW h, the ISO set the penalty $\theta^1_{j,h}, h \in \mathscr{H}$ to $\frac{1-\beta_j}{1-\beta_j^{ISO}}\vartheta^c = 4$ \$/MW h. Furthermore, Fig. 10(b) and (c) shows the value

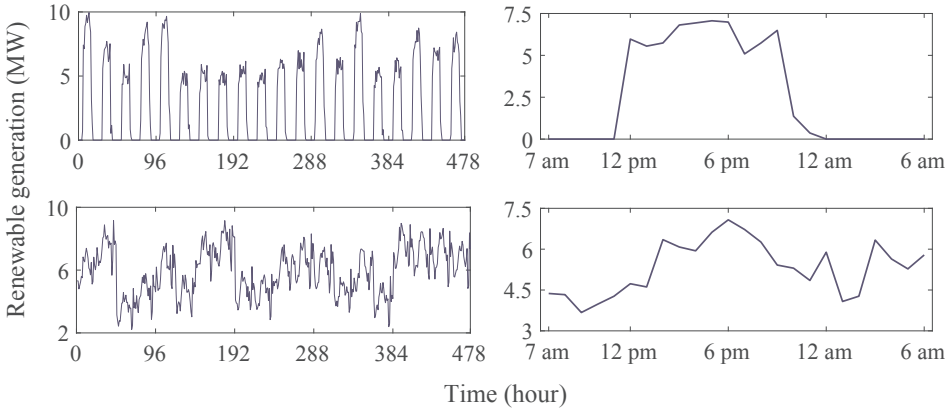

Fig. 4. (left figures) The PV panel and wind turbine historical data samples. (right figures) The presumed output power of the PV panel and wind turbine in buses 11 and 13.

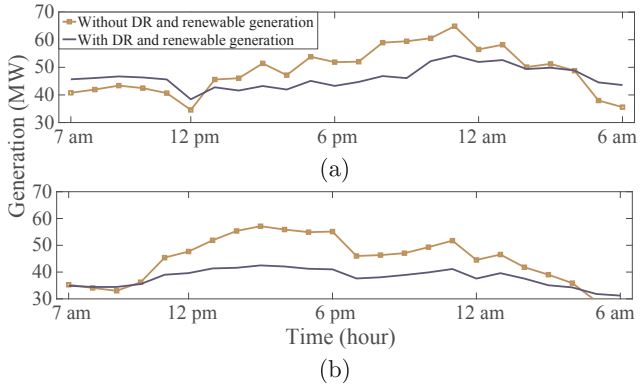

Fig. 6. The generation profile of the generators (a) 11 and (b) 13.

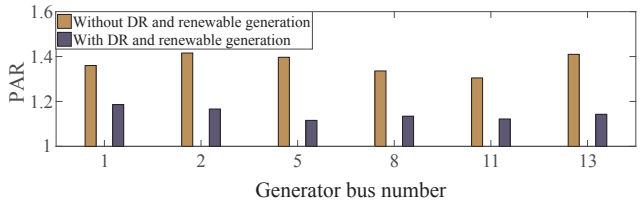

Fig. 7. The PAR in the generation of the generators with and without DR and renewable generation.

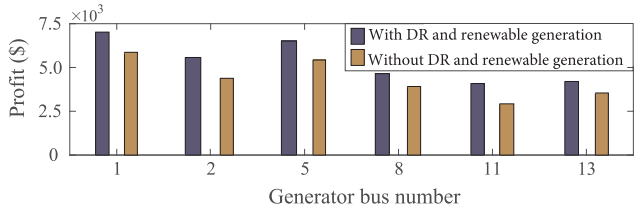

Fig. 8. The profit of the generators with and without DR and renewable generation.

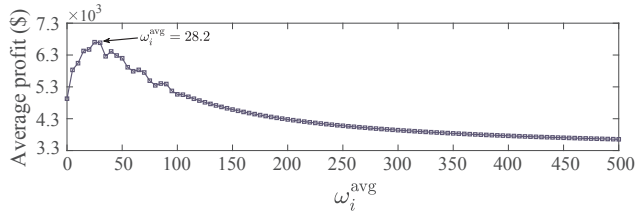

Fig. 9. The average profit of the generators in terms of the average weight coefficients $\omega_i^{\text{avg}}, i \in \mathscr{I}$.

of base payment/reward $\theta_{j,h}^2, h \in \mathscr{H}$ for generators in buses 11 and 13, respectively. Since the ISO is more risk averse than the generators, the value of $\theta_{j,h}^2 = \left[1-\left(\frac{\vartheta^c(1-\beta_j)}{1-\beta_j^{\text{ISO}}} + \frac{(\vartheta^c-1)(1-\beta_j)}{\frac{1}{K_j}\sum_{k\in\mathscr{K}_j}\gamma_j^{\text{ISO}}}\right)\right]\alpha_{j,h}$ is negative. That is, the ISO rewarded the generators, and the amount of reward is proportional to the threshold cost $\alpha_{j,h}$ in order to motivate the generators to become more risk averse. Using $\theta_{j,h}^1$ and $\theta_{j,h}^2, h \in \mathscr{H}$, the ISO can manipulate the risk attitude of the generators with renewable energies such that they behave similar to the ISO in the market.

4.6. Algorithm convergence and running time

We study the required number of iterations for our algorithm to converge, which can be interpreted as an indicator of the number of exchanged messages among the load aggregators, generators and the ISO. The value of the voltage angles depends on the decision variables of all generators and load aggregators. Thus, the convergence of the voltage angles is a viable indicator of the convergence of the decision variables in all buses of the system. Since the values of the voltage angles of all buses can be added by a constant, we illustrate the convergence of the phase angle difference between the voltages of the buses at the end nodes of the lines. For instance, we provide the convergence of $\delta_{1,5}-\delta_{2,5}$,$\delta_{7,10}-\delta_{5,10}$,$\delta_{28,15}-\delta_{6,15}$, and $\delta_{20,20}-\delta_{10,20}$ in Fig. 11. We can observe that 45 iterations are enough for convergence. The average running time of the algorithm for different initial conditions is 19 s for 200 random initial conditions.

We use MOSEK solver to solve the ISO's centralized problem (11). The solution is the same as the decentralized approach, but the running time is 35 s. In order to further elaborate the comparison, we provide the average running time of Algorithm 1 and the centralized approach for six test systems [48] in Fig. 12. The significant lower running time of the decentralized approach is due to the parallel update of the load aggregators and generators, as well as smaller number of decision variables in their local problems.

4.7. Comparing with the ADMM-based algorithm

One can also propose an ADMM-based algorithm [50] that still works with the partial Lagrange relaxation of the objective function (10) given in (24), but with an additional penalty term, referred to as *augmentation*. Details on implementing the ADMM-based decentralized algorithm can be found in [50]. In a nutshell, for the ADMM-based algorithm, the ISO, first, broadcasts both the price signals and the generation level of the generators to the load aggregators. After receiving the updated load demands from all load aggregators, the ISO communicates both the price signals and the updated load aggeragtors' demands to the generators. By receiving the updated generation level of the generators, the ISO updates the price signals, and the next iteration proceeds following the same iterative procedure. In Section 4, we will compare the performance of Algorithm 1 with the ADMM-based algorithm. In general, the ADMM-based algorithm can converge in a smaller number of iterations; nevertheless, the ISO needs to reveal the load aggregators' demand information to the generators, and the generation level of the generators to the load aggregators. Hence, the privacy of the entities may not be protected. Furthermore, the ISO should broadcast information two times (in series) to the entities in each iteration, which doubles the communication delay per iteration. The mentioned two drawbacks are important criteria, especially in a practical implementation of a decentralized algorithm.

We provide the average CPU time in Table 1. We emphasize that the ADMM algorithm converges to the solution of the centralized problem due to the convexity of the centralized problem and satisfying the Slater's conditions [50]. We can observe that the CPU time with the ADMM-based algorithm is lower than our proposed algorithm. Using the ADMM algorithm, however, the ISO needs to provide the load aggregators with some additional information about the decision making of the generators, and vice versa. This feature is not suitable for the energy markets, since the entities usually do not prefer to reveal their strategies to other competitors in the market.

5. Conclusion

In this paper, we proposed a decentralized algorithm for energy trading among load aggregators and generators in a power grid. In the proposed model, the ISO sends control signals to the entities to motivate

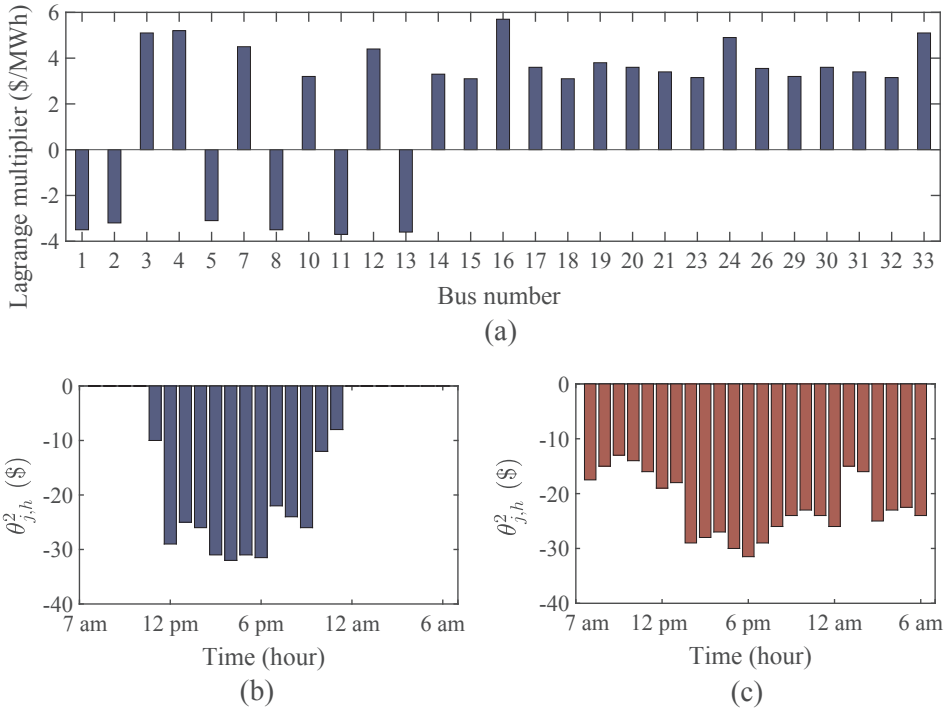

Fig. 10. (a) Lagrange multipliers in generator and load aggregator buses; (b) $\theta^2_{j,h}$ for the generator in bus 11; (c) $\theta^2_{j,h}$ for the generator in bus 13.

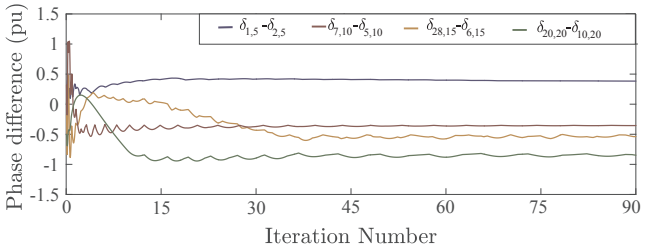

Fig. 11. The convergence of phase difference over transmission lines.

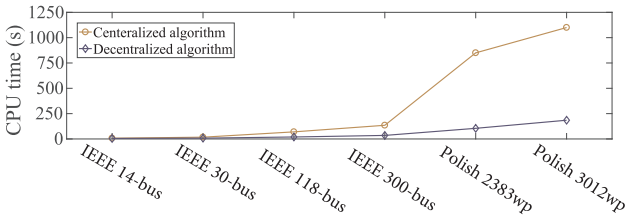

Fig. 12. The CPU time of the centralized and decentralized algorithms.

them towards optimizing their objectives independently, while meeting the physical constraints of the power network. We introduced the concept of CVaR to limit the likelihood of renewable generation shortage in the day-ahead market. In order to evaluate the performance of the proposed decentralized algorithm, we used an IEEE 30-bus test system connected to some renewable generators. Results confirmed that the algorithm converges in 45 iterations. We also evaluated the price responsive load profiles and generation values for various discomfort costs of the load aggregators, and verified that the proposed decentralized algorithm can benefit the load aggregators by reducing their cost by 18%, and the generators by reducing the PAR by 15% and increasing their profit by 17.1%. Our algorithm benefits the ISO by maintaining the privacy issues and a lower computational time compared to the centralized approach.

Table 1
The average CPU time for our proposed decentralized algorithm and the ADMM-based algorithm.

Test system	Algorithm 1 CPU time(s)	ADMM-based algorithm CPU time(s)
IEEE 14-bus	10.7	7.9
IEEE 30-bus	16.8	12.1
IEEE 118-bus	25.6	18.5
IEEE 300-bus	42.5	27.6
Polish 2383wp	136.3	104.1
Polish 3012wp	182.4	134.8

Appendix A. Load demand characteristics

Although load aggregator i considers the scheduling horizon $\mathscr{H}_{a,i} \subseteq \mathscr{H}$ to schedule each load $a \in \mathscr{A}_i$, different loads have different characteristics. We divide the set of loads in bus i into set $\mathscr{A}_i^1 \subseteq \mathscr{A}_i$ of loads of type 1 and set $\mathscr{A}_i^2 \subseteq \mathscr{A}_i$ of loads of type 2. A load of type 1 has a hard deadline. That is, it should be operated within the scheduling horizon and turned off in other time slots. Examples include the household's electric vehicle (EV) and production line of an industry. A load of type 2 is more flexible, and can be operated in the time slots out of the scheduling horizon, but at the cost of a relatively high discomfort for the consumer, e.g., the lighting in households, packing process in industries, and air conditioner in commercial buildings.

Considering the demands $x_{a,i,h}$ of loads $a \in \mathscr{A}_i$ in time slots $h \in \mathscr{H}$ as the decision variables for load aggregator i, we have the following operational constraints:

$$x_{a,i,h} = 0, \quad a \in \mathscr{A}_i^1, \quad h \notin \mathscr{H}_{a,i}, \tag{21a}$$

$$x_{a,i,h} \geqslant 0, \quad a \in \mathscr{A}_i^2, \quad h \notin \mathscr{H}_{a,i}, \tag{21b}$$

$$x_{a,i,h}^{\min} \leqslant x_{a,i,h} \leqslant x_{a,i,h}^{\max}, \quad a \in \mathscr{A}_i^1 \cup \mathscr{A}_i^2, \quad h \in \mathscr{H}_{a,i}, \tag{21c}$$

$$X_{a,i,h}^{\min} \leqslant \sum_{h \in \mathscr{H}} x_{a,i,h} \leqslant X_{a,i,h}^{\max}, \quad a \in \mathscr{A}_i^1 \cup \mathscr{A}_i^2. \tag{21d}$$

Constraints (21a) and (21b) are obtained from the flexibility of loads of types 1 and 2, respectively. Constrain (31a) indicates limited demand variation for load a in time slot h. Constrain (31b) indicates limited total energy demand of load a to complete its task.

Scheduling the loads usually results in a discomfort cost for the consumers of the load aggregator i. The discomfort cost for type 1 loads depends only on the total power consumption deviation from the desirable value (e.g., a consumer cares about the total charging level of its EV). For the scheduled power consumption profile $\boldsymbol{x}_{a,i} = (x_{a,i,h}, h \in \mathscr{H})$ and desirable profile $\boldsymbol{x}_{a,i}^{\text{des}} = (x_{a,i,h}^{\text{des}}, h \in \mathscr{H})$, a viable candidate for the discomfort cost of loads of type 1 is

$$\Omega_{a,i}(\boldsymbol{x}_{a,i}) = \omega_{a,i} \sum_{h \in \mathscr{H}_{a,i}} (x_{a,i,h} - x_{a,i,h}^{\text{des}})^2, \quad a \in \mathscr{A}_i^1, \tag{22}$$

where $\omega_{a,i}$ in cents/(kW)^2 is a nonnegative constant. The discomfort cost for type 2 loads depends on both the amount of power consumption and the time of consuming the power. The following discomfort cost function is a viable candidate:

$$\Omega_{a,i}(\boldsymbol{x}_{a,i}) = \sum_{h \in \mathscr{H}_{a,i}} \omega_{a,i,h} (x_{a,i,h} - x_{a,i,h}^{\text{des}})^2 + \sum_{h \notin \mathscr{H}_{a,i}} \omega'_{a,i,h} x_{a,i,h}, \quad a \in \mathscr{A}_i^2, \tag{23}$$

where $\omega_{a,i,h}$ in cents/(kW)^2 and $\omega'_{a,i,h} \gg \omega_{a,i,h}$ in cents/kW are *time dependent* nonnegative coefficients.

Appendix B. Proof of Theorem 1

Our proof involves two steps. We first show that (11) is a convex optimization problem with closed and bounded feasible space. Second, we show that the objective function (10) is lower bounded. Consequently, if problem (11) has a feasible solution, then it will have a unique minimizer.

The objective function (10) is convex with respect to variable vector $\boldsymbol{\psi}^{\text{ISO}}$, because the discomfort cost $\Omega_i(\boldsymbol{x}_i) = \sum_{a \in \mathscr{A}_i} \Omega_{a,i}(\boldsymbol{x}_{a,i})$ is a quadratic function (and thus a convex function) of $\boldsymbol{x}_{a,i}$ and the generation cost function $C_{j,h}^{\text{conv}}(p_{j,h}^{\text{conv}})$ is a convex function for (2). Furthermore, the approximate CVaR function $\widetilde{\mathscr{C}}_{j,h}^{\beta_j^{\text{ISO}}}(\boldsymbol{\eta}_{j,h}^{\text{ISO}}, \alpha_{j,h}^{\text{ISO}})$ is convex. The constraints of problem (11) are all linear, and by considering one bus as a slack bus (e.g., bus 1 with $\delta_{1,h} = 0, h \in \mathscr{H}$), the feasible space would be closed and bounded. Therefore, problem (11) is a convex optimization problem.

All terms in the objective function (10) are nonnegative, and thus the objective function (10) is lower bounded by zero. The proof is completed. ■.

Appendix C. Proof of Theorem 2

We define the vectors $\boldsymbol{x} = (\boldsymbol{x}_i, i \in \mathscr{I}), \boldsymbol{p}^{\text{conv}} = (\boldsymbol{p}_j^{\text{conv}}, j \in \mathscr{J}), \boldsymbol{p}^{\text{ren}} = (\boldsymbol{p}_j^{\text{ren}}, j \in \mathscr{J}), \boldsymbol{\delta} = (\boldsymbol{\delta}_h, h \in \mathscr{H})$, and $\boldsymbol{\alpha}^{\text{ISO}} = (\alpha_{j,h}^{\text{ISO}}, j \in \mathscr{J}, h \in \mathscr{H})$. Using the defined Lagrange multipliers, we can rewrite the partial Lagrange relaxation of the objective function (10) in the ISO's centralized problem (11) as follows:

$$\begin{aligned} f_{\text{Lag}}^{\text{ISO}}(\boldsymbol{x}, \boldsymbol{p}^{\text{conv}}, \boldsymbol{p}^{\text{ren}}, \boldsymbol{\alpha}^{\text{ISO}}, \boldsymbol{\delta}, \boldsymbol{\Lambda}) = & \sum_{i \in \mathscr{I}} \Omega_i(\boldsymbol{x}_i) + \sum_{h \in \mathscr{H}} \sum_{j \in \mathscr{J}} (C_{j,h}^{\text{conv}}(p_{j,h}^{\text{conv}}) + \vartheta^{\text{c}} \widetilde{\mathscr{C}}_{j,h}^{\beta_j^{\text{ISO}}}(p_{j,h}^{\text{ren}}, \alpha_{j,h}^{\text{ISO}})) + \sum_{i \in \mathscr{I}} \sum_{h \in \mathscr{H}} \lambda_{i,h}^{\text{agg}} \left(l_{i,h} + \sum_{(i,r) \in \mathscr{L}} b_{i,r}(\delta_{i,h} - \delta_{r,h}) \right) \\ & + \sum_{j \in \mathscr{J}} \sum_{h \in \mathscr{H}} \lambda_{j,h}^{\text{gen}} \left(p_{j,h}^{\text{conv}} + p_{j,h}^{\text{ren}} - \sum_{(j,r) \in \mathscr{L}} b_{j,r}(\delta_{j,h} - \delta_{r,h}) \right). \end{aligned} \tag{24}$$

The dual function is obtained as the minimum of $f_{\text{Lag}}^{\text{ISO}}(\cdot)$ over the variables $\boldsymbol{x}, \boldsymbol{p}^{\text{conv}}, \boldsymbol{p}^{\text{ren}}$, and $\boldsymbol{\alpha}^{\text{ISO}}$. That is, we have

$$\begin{aligned} f_{\text{Dual}}^{\text{ISO}}(\boldsymbol{\delta}, \boldsymbol{\Lambda}) = & \sum_{i \in \mathscr{I}} \min_{\boldsymbol{x}_i \in \mathscr{X}_i} \left\{ \Omega_i(\boldsymbol{x}_i) + \sum_{h \in \mathscr{H}} \lambda_{i,h}^{\text{agg}} l_{i,h} \right\} + \sum_{j \in \mathscr{J}} \min_{\substack{\boldsymbol{p}_j^{\text{conv}}, \boldsymbol{p}_j^{\text{ren}} \in \Phi_j, \\ \alpha_{j,h}^{\text{ISO}} \geqslant 0}} \left\{ \sum_{h \in \mathscr{H}} (\lambda_{j,h}^{\text{gen}}(p_{j,h}^{\text{conv}} + p_{j,h}^{\text{ren}}) + C_{j,h}^{\text{conv}}(p_{j,h}^{\text{conv}}) + \vartheta^{\text{c}} \widetilde{\mathscr{C}}_{j,h}^{\beta_j^{\text{ISO}}}(p_{j,h}^{\text{ren}}, \alpha_{j,h}^{\text{ISO}})) \right\} \\ & + \sum_{i \in \mathscr{I}} \sum_{h \in \mathscr{H}} \lambda_{i,h}^{\text{agg}} \left(\sum_{(i,r) \in \mathscr{L}} b_{i,r}(\delta_{i,h} - \delta_{r,h}) \right) + \sum_{j \in \mathscr{J}} \sum_{h \in \mathscr{H}} \lambda_{j,h}^{\text{gen}} \left(- \sum_{(j,r) \in \mathscr{L}} b_{j,r}(\delta_{j,h} - \delta_{r,h}) \right). \end{aligned} \tag{25}$$

The dual problem of the ISO's centralized problem is

$$\underset{\boldsymbol{\delta}, \boldsymbol{\Lambda}}{\text{maximize}} \quad f_{\text{Dual}}^{\text{ISO}}(\boldsymbol{\delta}, \boldsymbol{\Lambda}) \tag{26}$$

$$\text{subject to} \quad |b_{r,s}(\delta_{r,h} - \delta_{s,h})| \leqslant p_{r,s}^{\max}, (r,s) \in \mathscr{L}, \quad h \in \mathscr{H}, \tag{27}$$

$$\delta_{1,h} = 0, h \in \mathscr{H}. \tag{28}$$

Under the convexity assumption and Slater's condition, it can be shown that the optimal solution for the centralized problem is equal to the optimal solution for the Lagrange dual problem (26). The equilibrium $\mathscr{E}^{\star}(\boldsymbol{\rho}, \boldsymbol{\theta})$ will coincide with the unique solution to the ISO's centralized problem in (11) if and only if the KKT optimality conditions for the dual problem (26) of the ISO becomes the same as the optimality condition for the load aggregators and generators problems in (18) and (16).

For the first minimization problem in the dual function (25) for load aggregator i, we have

$$\frac{\partial C_i^{\text{agg}}(\boldsymbol{x}_i)}{\partial x_{i,h}} = \frac{\partial f_{\text{Dual}}^{\text{ISO}}(\boldsymbol{\delta},\boldsymbol{\Lambda})}{\partial x_{i,h}}. \tag{29}$$

Thus, we have

$$\rho_{i,h}^{*} = \lambda_{i,h}^{\text{agg},*}, \qquad i \in \mathscr{I}, \quad h \in \mathscr{H}. \tag{30}$$

For the second minimization problem in the dual function (25) for generator j, we have

$$\frac{\partial \pi_j^{\text{gen}}(\psi_j)}{\partial p_{j,h}^{\text{conv}}} = -\frac{\partial f_{\text{Dual}}^{\text{ISO}}(\boldsymbol{\delta},\boldsymbol{\Lambda})}{\partial p_{j,h}^{\text{conv}}}, \tag{31a}$$

$$\frac{\partial \pi_j^{\text{gen}}(\psi_j)}{\partial p_{j,h}^{\text{ren}}} = -\frac{\partial f_{\text{Dual}}^{\text{ISO}}(\boldsymbol{\delta},\boldsymbol{\Lambda})}{\partial p_{j,h}^{\text{ren}}}. \tag{31b}$$

$$\frac{\partial \pi_j^{\text{gen}}(\psi_j)}{\partial \alpha_{j,h}} = -\frac{\partial f_{\text{Dual}}^{\text{ISO}}(\boldsymbol{\delta},\boldsymbol{\Lambda})}{\partial \alpha_{j,h}^{\text{ISO}}}. \tag{31c}$$

Note that, the local problem of generator j in (16) is different from the second minimization problem in the ISO's dual function in (25). First, problem (16) is a maximization problem, and thus we have used a negative sign in the right-hand side of (31a)–(31c). Second, the CVaR function $\widetilde{\mathscr{C}}_{j,h}^{\beta_j}(p_{j,h}^{\text{ren}},\alpha_{j,h})$ of the generator j in (14) is different from the CVaR function $\widetilde{\mathscr{C}}_{j,h}^{\beta_j^{\text{ISO}}}(p_{j,h}^{\text{ren}},\alpha_{j,h}^{\text{ISO}})$ of the ISO in (7) due to differences in the β_j and β_j^{ISO}, as well as the penalty functions $\Delta_{j,h}(\cdot)$ in (12) and $\Delta_{j,h}^{\text{ISO}}(\cdot)$ in (3). From (31a), we have

$$\rho_{j,h}^{*} - \frac{\partial C_{j,h}(p_{j,h}^{\text{conv}})}{\partial p_{j,h}^{\text{conv}}} = -\lambda_{j,h}^{\text{gen},*} - \frac{\partial C_{j,h}(p_{j,h}^{\text{conv}})}{\partial p_{j,h}^{\text{conv}}}, \tag{32}$$

which is equivalent to

$$\rho_{j,h}^{*} = -\lambda_{j,h}^{\text{gen},*}, \qquad j \in \mathscr{J}, \quad h \in \mathscr{H}. \tag{33}$$

We assume that $\theta_{j,h}^{2,*} = \eta_{j,h}^{*}\alpha_{j,h}^{*}$. From (31b) and (31c), we have

$$\frac{\theta_{j,h}^{1,*}}{K_j(1-\beta_j)} \sum_{k\in\mathscr{K}_j} \gamma_{j,h}^{k,*} = \frac{\vartheta^c}{K_j(1-\beta_j^{\text{ISO}})} \sum_{k\in\mathscr{K}_j} \gamma_{j,h}^{\text{ISO},k,*}, \tag{34a}$$

$$1 - \frac{(1-\eta_{j,h}^{*})\sum_{k\in\mathscr{K}_j}\gamma_{j,h}^{k,*}}{K_j(1-\beta_j)} = \vartheta^c - \frac{\vartheta^c \sum_{k\in\mathscr{K}_j}\gamma_{j,h}^{\text{ISO},k,*}}{K_j(1-\beta_j^{\text{ISO}})}. \tag{34b}$$

From (34a), we have

$$\theta_{j,h}^{1,*} = \vartheta^c \frac{1-\beta_j}{1-\beta_j^{\text{ISO}}}. \tag{35}$$

From (34b), we have

$$\eta_{j,h}^{*} = 1 - \left(\frac{\vartheta^c(1-\beta_j)}{1-\beta_j^{\text{ISO}}} + \frac{(\vartheta^c-1)(1-\beta_j)}{\frac{1}{K_j}\sum_{k\in\mathscr{K}_j}\gamma_j^{\text{ISO},k,*}} \right), \tag{36}$$

and thus, we obtain

$$\theta_{j,h}^{2} = \left[1 - \left(\frac{\vartheta^c(1-\beta_j)}{1-\beta_j^{\text{ISO}}} + \frac{(\vartheta^c-1)(1-\beta_j)}{\frac{1}{K_j}\sum_{k\in\mathscr{K}_j}\gamma_j^{\text{ISO},k,*}} \right) \right] \alpha_{j,h}^{*}. \tag{37}$$

Consequently, the ISO needs to send the price signals in (19a)–(19d) to the load aggregators and generators. Then, the ISO should solve its dual problem in (26) using the updated demand and generation level of the entities. In other words, the ISO will update the voltage angles $\boldsymbol{\delta}$ and Lagrange multipliers $\boldsymbol{\Lambda}$ using the update process in (20a) and (20b). The proof is completed. ■

References

[1] Kar S, Hug G, Mohammadi J, Moura JM. Distributed state estimation and energy management in smart grids: a consensus innovations approach. IEEE J Sel Top Sign Process 2014;8(6):1022–38.

[2] Amini M, Frye J, Ilić MD, Karabasoglu O. Smart residential energy scheduling utilizing two stage mixed integer linear programming. In: North American power symposium (NAPS); 2015. p. 1–6.

[3] Qadrdan M, Cheng M, Wu J, Jenkins N. Benefits of demand-side response in combined gas and electricity networks. Appl Energy 2017;192:360–9.

[4] Drysdale B, Wu J, Jenkins N. Flexible demand in the gb domestic electricity sector in 2030. Appl Energy 2015;139:281–90.

[5] Chai B, Chen J, Yang Z, Zhang Y. Demand response management with multiple utility companies: a two-level game approach. IEEE Trans Smart Grid 2014;5(2):722–31.

[6] Bahrami S, Wong VW, Huang J. An online learning algorithm for demand response in smart grid. IEEE Trans Smart Grid 2017. http://dx.doi.org/10.1109/TSG.2017.2667599.
[7] Maharjan S, Zhu Q, Zhang Y, Gjessing S, Basar T. Dependable demand response management in the smart grid: a Stackelberg game approach. IEEE Trans Smart Grid 2013;4(1):120–32.
[8] Deng R, Yang Z, Hou F, Chow M-Y, Chen J. Distributed real-time demand response in multiseller-multibuyer smart distribution grid. IEEE Trans Power Syst 2014(99):1–11.
[9] Amini MH, et al. Sustainable Interdependent Networks. Springer; 2018.
[10] Amini MH, Nabi B, Haghifam M-R. Load management using multi-agent systems in smart distribution network. In: IEEE power and energy society general meeting (PES); 2013. p. 1–5.
[11] Shahmohammadi A, Sioshansi R, Conejo AJ, Afsharnia S. Market equilibria and interactions between strategic generation, wind, and storage. Appl Energy 2017. http://dx.doi.org/10.1016/j.apenergy.2017.10.035.
[12] Parvania M, Fotuhi-Firuzabad M, Shahidehpour M. ISO's optimal strategies for scheduling the hourly demand response in day-ahead markets. IEEE Trans Power Syst 2014;29(6):2636–45.
[13] Boroojeni KG, Amini MH, Bahrami S, Iyengar S, Sarwat AI, Karabasoglu O. A novel multi-time-scale modeling for electric power demand forecasting: from short-term to medium-term horizon. Electr Power Syst Res 2017;142:58–73.
[14] Disfani VR, Fan L, Miao Z. Distributed DC optimal power flow for radial networks through partial primal dual algorithm. 2015 IEEE power & energy society general meeting. IEEE; 2015. p. 1–5.
[15] Shi W, Li N, Xie X, Chu C, Gadh R. Optimal residential demand response in distribution networks. IEEE J Sel Areas Commun 2014;32(7):1441–50.
[16] Li N, Gan L, Chen L, Low S. An optimization-based demand response in radial distribution networks. In: Proc of IEEE Globecom, Anaheim, CA; 2012.
[17] Dall'Anese E, Zhu H, Giannakis GB. Distributed optimal power flow for smart microgrids. IEEE Trans Smart Grid 2013;4(3):1464–75.
[18] Bakirtzis AG, Biskas PN. A decentralized solution to the DC-OPF of interconnected power systems. IEEE Trans Power Syst 2003;18(3):1007–13.
[19] Erseghe T. Distributed optimal power flow using ADMM. IEEE Trans Power Syst 2014;29(5):2370–80.
[20] Peng Q, Low SH. Distributed algorithm for optimal power flow on a radial network. In: Proc of IEEE conf on decision and control; 2014. p. 167–72.
[21] Magnússon S, Weeraddana PC, Fischione C. A distributed approach for the optimal power-flow problem based on ADMM and sequential convex approximations. IEEE Trans Contr Netw Syst 2015;2(3):238–53.
[22] Mohammadi A, Mehrtash M, Kargarian A. Diagonal quadratic approximation for decentralized collaborative TSO + DSO optimal power flow. IEEE Trans Smart Grid 2018. http://dx.doi.org/10.1109/TSG.2018.2796034.
[23] Arroyo JM, Galiana FD. Energy and reserve pricing in security and network-constrained electricity markets. IEEE Trans Power Syst 2005;20(2):634–43.
[24] Hug-Glanzmann G, Andersson G. Decentralized optimal power flow control for overlapping areas in power systems. IEEE Trans Power Syst 2009;24(1):327–36.
[25] Amini MH, Jaddivada R, Mishra S, Karabasoglu O. Distributed security constrained economic dispatch. Innovative smart grid technologies-Asia. IEEE; 2015. p. 1–6.
[26] Zhang H, Li P. Chance constrained programming for optimal power flow under uncertainty. IEEE Trans Power Syst 2011;26(4):2417–24.
[27] Bienstock D, Chertkov M, Harnett S. Chance-constrained optimal power flow: risk-aware network control under uncertainty. SIAM Rev 2014;56(3):461–95.
[28] Cao Y, Tan Y, Li C, Rehtanz C. Chance-constrained optimization-based unbalanced optimal power flow for radial distribution networks. IEEE Trans Power Deliv 2013;28(3):1855–64.
[29] Jabr RA. Adjustable robust OPF with renewable energy sources. IEEE Trans Power Syst 2013;28(4):4742–51.
[30] Miranda V, Saraiva J. Fuzzy modelling of power system optimal load flow. Power industry computer application conference, 1991. Conference proceedings. IEEE; 1991. p. 386–92.
[31] Nasri A, Kazempour SJ, Conejo AJ, Ghandhari M. Network-constrained ac unit commitment under uncertainty: a Benders' decomposition approach. IEEE Trans Power Syst 2016;31(1):412–22.
[32] Zhou Y, Wang C, Wu J, Wang J, Cheng M, Li G. Optimal scheduling of aggregated thermostatically controlled loads with renewable generation in the intraday electricity market. Appl Energy 2017;188:456–65.
[33] Zhang Y, Giannakis GB. Robust optimal power flow with wind integration using conditional value-at-risk. Smart grid communications (SmartGridComm). IEEE; 2013. p. 654–9.
[34] Samadi P, Bahrami S, Wong V, Schober R. Power dispatch and load control with generation uncertainty. In: Proc of IEEE global conf on signal and information processing (GlobalSIP); 2015. p. 1126–30.
[35] Vithayasrichareon P, Riesz J, MacGill I. Operational flexibility of future generation portfolios with high renewables. Appl Energy 2017;206:32–41.
[36] Bahrami S, Wong VWS. Security-constrained unit commitment for ac-dc grids with generation and load uncertainty. IEEE Trans Power Syst 2017. http://dx.doi.org/10.1109/TPWRS.2017.2749303.
[37] González-Aparicio I, Zucker A. Impact of wind power uncertainty forecasting on the market integration of wind energy in Spain. Appl Energy 2015;159:334–49.
[38] Bahrami S, Amini MH, Shafie-khah M, Catalao JP. A decentralized electricity market scheme enabling demand response deployment. IEEE Trans Power Syst 2017. http://dx.doi.org/10.1109/TPWRS.2017.2771279.
[39] Somarakis C, Siami M, Motee N. Interplays between systemic risk and network topology in consensus networks. IFAC-PapersOnLine 2016;49(22):333–8.
[40] Somarakis C, Ghaedsharaf Y, Motee N. Aggregate fluctuations in time-delay linear consensus networks: a systemic risk perspective. In: American control conference (ACC); 2017. p. 2351–6.
[41] Li T, Shahidehpour M. Price-based unit commitment: a case of lagrangian relaxation versus mixed integer programming. IEEE Trans Power Syst 2005;20(4):2015–25.
[42] Stewart J. Calculus. 4th ed. CA: Brooks/Cole Pub Co.; 1999.
[43] Rockafellar RT, Uryasev S. Optimization of conditional value-at-risk. J Risk 2000;2:21–42.
[44] Overbye TJ, Cheng X, Sun Y. A comparison of the AC and DC power flow models for LMP calculations. Proceedings of the 37th annual Hawaii international conference on system sciences. IEEE; 2004.
[45] Stott B, Jardim J, Alsaç O. DC power flow revisited. IEEE Trans Power Syst 2009;24(3):1290–300.
[46] Kleywegt AJ, Shapiro A, Homem-De-Mello T. The sample average approximation method for stochastic discrete optimization. SIAM J Optimiz 2001;12(2):479–502.
[47] Bertsekas DP. Nonlinear programming. 2nd ed. Belmont (Massachusetts): Athena scientific; 1999.
[48] University of Washington, power systems test case archive. URL < http://www.ee.washington.edu/research/pstca > .
[49] Independent Electricity System Operator (IESO). URL < http://www.ieso.ca > .
[50] Boyd S, Parikh N, Chu E, Peleato B, Eckstein J. Distributed optimization and statistical learning via the alternating direction method of multipliers. Found Trends Mach Learn 2011;3(1):1–122.